Time-dependent partial waves and vortex rings in the dynamics of wavepackets

1997 J. Phys. A: Math. Gen. 30 5381

(http://iopscience.iop.org/0305-4470/30/15/023)

J. Phys. A: Math. Gen. **30** (1997) 5381–5392. Printed in the UK PII: S0305-4470(97)81929-4

Time-dependent partial waves and vortex rings in the dynamics of wavepackets

R Arvieu†, P Rozmej‡§ and W Berej‡

† Institut des Sciences Nucléaires, F 38026 Grenoble-Cedex, France
‡ Theoretical Physics Department, University MCS, 20-031 Lublin, Poland

Received 18 February 1997, in final form 24 April 1997

Abstract. We find a new class of time-dependent partial waves which are solutions of the time-dependent Schrödinger equation for three-dimensional harmonic oscillator. We also show the decomposition of coherent states of harmonic oscillator into these partial waves. This decomposition appears to be particularly convenient for a description of the dynamics of a wavepacket representing a particle with spin when the spin–orbit interaction is present in the Hamiltonian. An example of an evolution of a localized wavepacket into a torus and backwards, for particular initial conditions is analysed in analytical terms and shown with computer graphics.

1. Introduction

The rapid technological development of short-pulsed lasers during the last decade has made it possible to produce and detect particular states, coherent superpositions of stationary electron states for a wide variety of physical systems. The dynamics of these initially well localized wavepackets is a subject of much current investigation in many areas of physics and chemistry [1, 2]. Extensive research by means of both theoretical and experimental methods has brought about an understanding of the intriguing phenomena of a hierarchy of collapses and revivals for particularly prepared wavepackets in the Jaynes–Cummings model (JCM) of quantum optics [3–7] and in Rydberg atoms [8–14].

In this paper we construct new solutions to the time-dependent Schrödinger equation for spherical harmonic oscillator (HO). We use these solutions further to describe the evolution of wavepackets representing a particle with spin moving in HO potential with an additional spin–orbit interaction. Time-dependent partial waves allow a much clearer interpretation of subtle interference effects as well as for a substantial acceleration of numerical codes used for graphical presentation of a complicated wavepacket motion.

This paper is organized as follows. In section 2 we construct time-dependent partial waves for the harmonic oscillator and show the decomposition of coherent states into these states. In section 3 we show the motion of individual partial waves. In section 4 we discuss time-dependent spinors corresponding to solutions of the time-dependent Schrödinger equation for a Hamiltonian containing a spin–orbit interaction and show a possibility of evolution of an initially localized wavepacket into a toroidal shape and backwards. Sections 5 and 6 present graphical illustrations of the wavepacket motion and conclusions.

§ To whom correspondence should be addressed.

0305-4470/97/155381+12$19.50

2. Time-dependent partial waves for the harmonic oscillator

It is not so well known that there exist simple time-dependent partial waves which are solutions of the Schrödinger equation of the three-dimensional oscillator. The proof will be given below.

We look for solutions $\psi_l^m(\boldsymbol{r},t)$ of the time-dependent Schrödinger equation for the spherical harmonic oscillator (with $\hbar = m = \omega = 1$) with the following form

$$\psi_l^m(\boldsymbol{r},t) = F(t)\mathrm{e}^{-\frac{1}{2}r^2} W_l(R_0\mathrm{e}^{-\mathrm{i}t}r)Y_l^m(\theta,\varphi) \tag{1}$$

where $F(t)$ and W_l must be determined in terms of a complex number R_0.

We easily find that W_l must obey the differential equation

$$Z^2\frac{\mathrm{d}^2W_l}{\mathrm{d}Z^2} + 2Z\frac{\mathrm{d}W_l}{\mathrm{d}Z} - \left[l(l+1) + \left(3 - \frac{2\mathrm{i}}{F}\frac{\mathrm{d}F}{\mathrm{d}t}\right)r^2\right]W_l = 0 \tag{2}$$

with a new variable Z

$$Z = R_0\mathrm{e}^{-\mathrm{i}t}r. \tag{3}$$

W_l depends only on this variable if F solves the equation

$$3 - \frac{2\mathrm{i}}{F}\frac{\mathrm{d}F}{\mathrm{d}t} = {R_0}^2\mathrm{e}^{-2\mathrm{i}t}. \tag{4}$$

Within an arbitrary constant factor, which is not written the solution is

$$F(t) = \mathrm{e}^{-\frac{3}{2}\mathrm{i}t}\mathrm{e}^{-\frac{1}{4}{R_0}^2\mathrm{e}^{-2\mathrm{i}t}}. \tag{5}$$

The equation solved by W_l becomes

$$Z^2\frac{\mathrm{d}^2W_l}{\mathrm{d}Z^2} + 2Z\frac{\mathrm{d}W_l}{\mathrm{d}Z} - [l(l+1) + Z^2]W_l = 0 \tag{6}$$

which is the equation for the modified spherical Bessel functions.

In the following we will use only the modified spherical Bessel functions of the first kind with the usual conventions of literature [15]

$$W_l(Z) = \sqrt{\frac{\pi}{2Z}}I_{l+\frac{1}{2}}(Z) \tag{7}$$

$$= \frac{Z^l}{(2l+1)!!}\left[1 + \frac{\frac{1}{2}Z^2}{1!(2l+3)} + \frac{(\frac{1}{2}Z^2)^2}{2!(2l+3)(2l+5)} + \cdots\right]. \tag{8}$$

The interpretation of these waves is very simple: there is an harmonic motion in the radial part of the wavefunction keeping the angular part the same because of angular momentum conservation.

The partial waves $\psi_l^m(\boldsymbol{r},t)$ just defined occur in a natural way in the expansion of a coherent time-dependent Gaussian wavepacket into partial waves. In such a wavepacket the constant R_0 finds its interpretation by combining the position of the centre of the wavepacket $\boldsymbol{r}_0$ to its mean momentum $\boldsymbol{p}_0$ at a time $t = 0$. Let $\boldsymbol{r}_t$ and $\boldsymbol{p}_t$ be such vectors at time t and let us define

$$\boldsymbol{R}_t = \boldsymbol{r}_t + \mathrm{i}\boldsymbol{p}_t \tag{9}$$

while

$$\boldsymbol{R}_0 = \boldsymbol{r}_0 + \mathrm{i}\boldsymbol{p}_0. \tag{10}$$

These two vectors are related by

$$\boldsymbol{R}_t = \boldsymbol{R}_0 \mathrm{e}^{-\mathrm{i}t}. \tag{11}$$

A normalized Gaussian wavepacket centred on $\boldsymbol{r}_t$ with mean momentum $\boldsymbol{p}_t$ is now written as

$$\bar{\psi}_{\boldsymbol{R}_t}(\boldsymbol{r}) = \pi^{-\frac{3}{4}} \mathrm{e}^{-\frac{1}{2}(\boldsymbol{r}-\boldsymbol{r}_t)^2} \mathrm{e}^{\mathrm{i}\boldsymbol{p}_t\cdot\boldsymbol{r}} = \pi^{-\frac{3}{4}} \mathrm{e}^{-\frac{1}{2}r^2} \mathrm{e}^{-\frac{1}{2}{r_t}^2} \mathrm{e}^{\boldsymbol{r}\cdot\boldsymbol{R}_t}. \tag{12}$$

Using 10.2.36 from [15] the modified Bessel function of the first kind of argument $Z = R_t r = R_0 \mathrm{e}^{-\mathrm{i}t} r$ appears in the expansion of the last exponential of (12)

$$\mathrm{e}^{\boldsymbol{r}\cdot\boldsymbol{R}_t} = \sum_{l=0}^{\infty} (2l+1) \sqrt{\frac{\pi}{2Z}}\, I_{l+\frac{1}{2}}(Z)\, P_l(\cos\Theta) \tag{13}$$

and R_0 is defined as

$$R_0 = (\boldsymbol{R}_0 \cdot \boldsymbol{R}_0)^{\frac{1}{2}} = ({r_0}^2 - {p_0}^2 + 2\mathrm{i}\boldsymbol{r}_0 \cdot \boldsymbol{p}_0)^{\frac{1}{2}}. \tag{14}$$

In a Gaussian wavepacket all the time-dependent partial waves share the same parameter R_0. However, it is possible to consider more general wavepacket for which R_0 might be different for different l.

The Legendre polynomial $P_l(\cos\Theta)$ depends on the (complex) angle Θ between $\boldsymbol{r}$ and $\boldsymbol{R}_t$. However, this angle is time independent. Indeed for each direction α, $\alpha = x, y, z$ one has

$$r_\alpha(t) + \mathrm{i}p_\alpha(t) = (r_\alpha(0) + \mathrm{i}p_\alpha(0))\mathrm{e}^{-\mathrm{i}t} \tag{15}$$

as well as equation (11), therefore

$$\begin{aligned} \cos(\Theta) &= \frac{x[x(t) + \mathrm{i}p_x(t)] + y[y(t) + \mathrm{i}p_y(t)] + z[z(t) + \mathrm{i}p_z(t)]}{R_t r} \\ &= \frac{x[x(0) + \mathrm{i}p_x(0)] + y[y(0) + \mathrm{i}p_y(0)] + z[z(0) + \mathrm{i}p_z(0)]}{R_0 r}. \end{aligned} \tag{16}$$

Then if the complex direction θ_{R_0}, φ_{R_0} of $\boldsymbol{R}_0$ is introduced through

$$\begin{aligned} \cos\theta_{R_0} &= \frac{z(0) + \mathrm{i}p_z(0)}{R_0} \\ \sin\theta_{R_0}\cos\varphi_{R_0} &= \frac{x(0) + \mathrm{i}p_x(0)}{R_0} \\ \sin\theta_{R_0}\sin\varphi_{R_0} &= \frac{y(0) + \mathrm{i}p_y(0)}{R_0} \end{aligned} \tag{17}$$

one writes the addition formula:

$$P_l(\cos\Theta) = \frac{4\pi}{2l+1} \sum_{m=-l}^{l} (-1)^m Y_l^m(\theta,\varphi) Y_l^{-m}(\theta_{R_0}, \varphi_{R_0}). \tag{18}$$

We can now rewrite $\bar{\psi}_{\boldsymbol{R}_t}$ as

$$\bar{\psi}_{\boldsymbol{R}_t}(\boldsymbol{r}) = 4\pi^{\frac{1}{4}} \mathrm{e}^{-\frac{1}{2}(r^2+r_t^2)} \sum_{l=0}^{\infty} \sum_{m=-l}^{l} (-1)^m Y_l^{-m}(\theta_{R_0}, \varphi_{R_0}) W_l(R_t r) Y_l^m(\theta,\varphi). \tag{19}$$

We will now extract the function F (5) in order to show explicitly the time-dependent partial waves

$$\begin{aligned} \mathrm{e}^{-\frac{1}{4}R_0^2 \mathrm{e}^{-2\mathrm{i}t}} &= \mathrm{e}^{-\frac{1}{4}(r_t^2 - p_t^2 + 2\mathrm{i}\boldsymbol{r}_t\cdot\boldsymbol{p}_t)} \\ &= \mathrm{e}^{-\frac{1}{2}r_t^2} \mathrm{e}^{-\frac{\mathrm{i}}{2}\boldsymbol{r}_t\cdot\boldsymbol{p}_t} \mathrm{e}^{\frac{E_0}{2}}. \end{aligned} \tag{20}$$

The classical energy $E_0 = \frac{r_0^2+p_0^2}{2}$ has been introduced above. The time-dependent partial waves (1) which appear in the Gaussian wavepacket at time t are then expressed as:

$$\psi_l^m(\boldsymbol{r}, t) = \mathrm{e}^{-(\frac{3}{2}\mathrm{i}t+\frac{1}{2}\boldsymbol{r}_t\cdot\boldsymbol{p}_t+\frac{r^2+r_t^2}{2}-\frac{E_0}{2})} W_l(R_t r) Y_l^m(\theta, \varphi). \tag{21}$$

The Gaussian wavepacket (19) can now be expressed as follows in terms of (21)

$$\bar{\psi}_{\boldsymbol{R}_t}(\boldsymbol{r}) = 4\pi^{\frac{1}{4}} \mathrm{e}^{\mathrm{i}(\frac{3}{2}t+\frac{r_t\cdot p_t}{2})-\frac{E_0}{2}} \sum_{lm} (-1)^m Y_l^{-m}(\theta_{R_0}, \varphi_{R_0}) \psi_l^m(\boldsymbol{r}, t). \tag{22}$$

Clearly one only obtains a solution of the Schrödinger equation if we change the phase. Let $\psi_{\boldsymbol{R}_t}(\boldsymbol{r})$ be this solution

$$\begin{aligned}\psi_{\boldsymbol{R}_t}(\boldsymbol{r}) &= \mathrm{e}^{-\mathrm{i}(\frac{3}{2}t+\frac{r_t\cdot p_t}{2})} \bar{\psi}_{\boldsymbol{R}_t}(\boldsymbol{r}) \\ &= \sum_{lm} (-1)^m 4\pi^{\frac{1}{4}} \mathrm{e}^{-\frac{E_0}{2}} Y_l^{-m}(\theta_{R_0}, \varphi_{R_0}) \psi_l^m(\boldsymbol{r}, t) \\ &= \sum_{lm} C_{lm}(\boldsymbol{R}_0) \psi_l^m(\boldsymbol{r}, t). \end{aligned} \tag{23}$$

The weight $C_{l_m}(\boldsymbol{R}_0)$ of the time-dependent partial wave $\psi_l^m(\boldsymbol{r}, t)$ is now seen to be

$$C_{lm}(\boldsymbol{R}_0) = (-1)^m 4\pi^{\frac{1}{4}} \mathrm{e}^{-\frac{E_0}{2}} Y_l^{-m}(\theta_{R_0}, \varphi_{R_0}). \tag{24}$$

An expansion similar to equation (23) is found in [16]. However, the time dependence of the radial function is lacking in this reference as well as the phase which is needed to correct the Gaussian wavepacket. Its first part contains the zero point energy of the quantum oscillator, while the second part: $\exp(-\mathrm{i}r_t p_t/2)$ is a well known phase difference between the coherent state of the harmonic oscillator and the displaced Gaussian (12) with average momentum p_t. It is a simple exercise to check that the wave written in the first line of (23) verifies the time-dependent Schrödinger equation while (12) does not. The existence of the second part of this phase is pointed out in some textbooks [17] in the static case but as we have proved here it can also be used in the time-dependent one provided one adds the zero point energy.

3. Representation of the time-dependent partial waves

Let us define the phase of R_0 by

$$R_0 = ({r_0}^2 - {p_0}^2 + 2\mathrm{i}\boldsymbol{r}_0 \cdot \boldsymbol{p}_0)^{\frac{1}{2}} = |R_0|\, \mathrm{e}^{\mathrm{i}\delta_0}. \tag{25}$$

The argument of the modified Bessel function is $Z = r|R_0|\mathrm{e}^{-\mathrm{i}(t-\delta_0)}$. Changing the initial conditions of the wavepacket produces a change of $|R_0|$ and δ_0. However, it is clear that the change of the phase can be taken into account in the radial partial wave $W_l(z)$ by a shift of the origin of time. It is therefore possible to analyse the different partial waves by assuming that $\delta_0 = 0$. This possibility arises if $p_0 = 0$, $R_0 = r_0$. For these values the Gaussian wavepacket performs a linear motion. It is striking that the radial motions of the partial waves corresponding to such a case contain all the proper information which can be used for all the different trajectories, i.e. circular or elliptical. The differences between the trajectories will be introduced by the coefficients $C_{lm}(\boldsymbol{R}_0)$.

In the following figures we have chosen to study the radial waves for the mean energy $E_0 = N = 20$, i.e. $r_0 = \sqrt{2E_0} = \sqrt{40} = R_0$. The eight lowest partial waves present in the development of a Gaussian wavepacket are represented in figure 1 (as a matter of fact we have represented the density multiplied by r^2) for a time range from $t = 0$ to $\frac{T}{2}$ (T is the

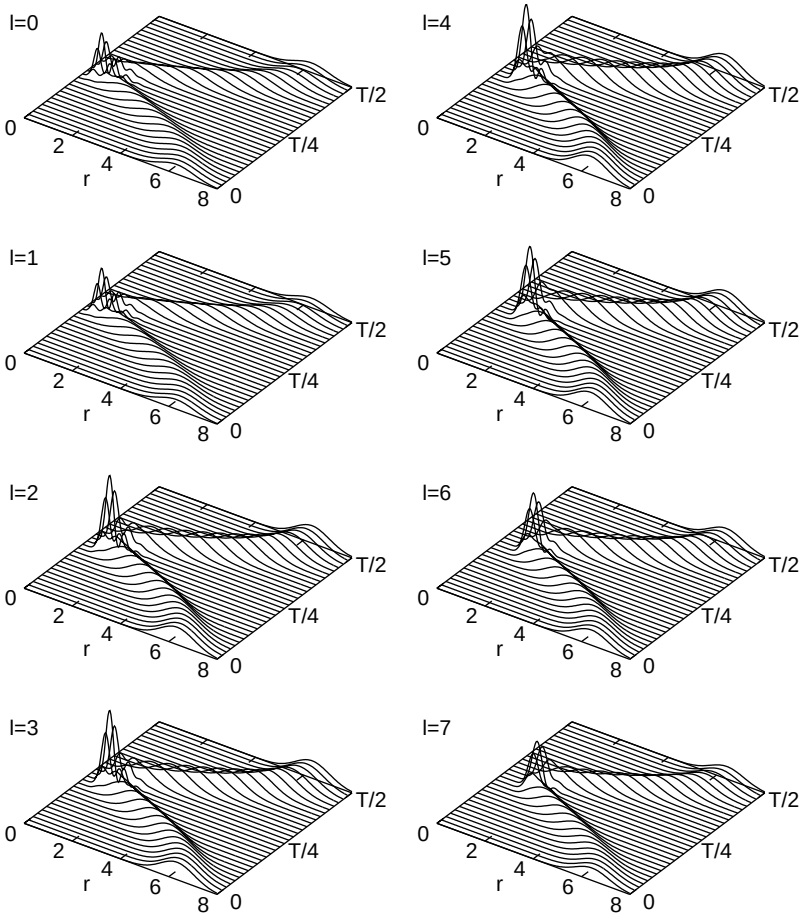

Figure 1. Radial motion of eight lowest partial partial waves with $l = 0, 1, \ldots, 7$ contributing to the linear motion of the Gaussian wavepacket. $|r\psi_l(r,t)|^2$ is shown as a function of r for 30 time steps in the interval $t \in [0, \frac{T}{2}]$. The case $E_0 = N = 20$ is presented. The vertical scale is the same for all figures.

harmonic oscillator period). The densities exhibit the same motion towards the origin and of course this radial motion is symmetric with respect to $t = \frac{T}{4}$. However, there is clearly an effect of the centrifugal barrier since the waves with the highest l are repelled from the origin. Also some secondary maxima are present. It is worth mentioning once again that the effects of the centrifugal barrier cancel when one adds the waves to produce a linear motion. We should also note that the spread of the partial waves does not depend on l in a significant manner.

In figure 2 the squares of 16 lowest partial waves ($|r\psi_l(r,t)|^2$) are represented as functions of r for $t = 0$. The concentration of the waves at the same r is spectacular. The intensity of the waves increases when l goes from $l = 0$ to $l = 4$ and decrease afterwards. In order to explain the concentration of the wave in three dimensions the angular part plays a role as will be discussed later.

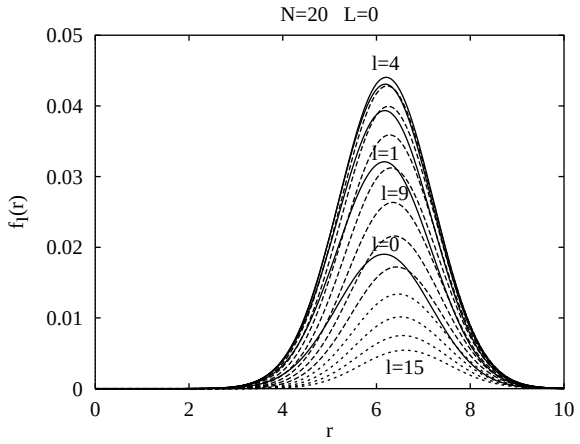

Figure 2. Decomposition of the Gaussian wavepacket into partial waves at $t = 0, r_0 = \sqrt{2N} = \sqrt{40}$. The lowest 16 partial waves with $l = 0, 1, \ldots, 15$ are shown. Waves with $l = 0$–4 are represented by full curves (intensity increases with l), those with $l = 5$–15 are represented by broken ones (their intensities decrease).

4. Time-dependent spinors

We will now study the evolution of a coherent wavepacket which is initially in a pure spin eigenstate chosen as $s_z = +\frac{1}{2}$. This wavepacket will evolve on the action of the harmonic oscillator evolution operator $U_0(t)$ and of the spin–orbit part $U_{ls}(t)$. As in our previous papers [18–22] we will use the spin–orbit Hamiltonian with a constant factor κ:

$$V_{ls} = \kappa(\boldsymbol{l} \cdot \boldsymbol{\sigma}) \tag{26}$$

and therefore U_0 commutes with V_{ls}. The Hamiltonian contains the ratio of the two timescales (let us recall that $\omega = 1$)

$$\frac{T_{ls}}{T} = \frac{2\pi}{\kappa}\frac{\omega}{2\pi} = \frac{1}{\kappa}. \tag{27}$$

The fully normalized spinor is written at time $t = 0$ as

$$\tilde{\psi}_{\boldsymbol{R}_0}(\boldsymbol{r}) = \begin{pmatrix} \psi_{\boldsymbol{R}_0}(\boldsymbol{r}) \\ 0 \end{pmatrix} = \sum_{lm} C_{lm}(\boldsymbol{R}_0) \begin{pmatrix} \psi_l^m(\boldsymbol{r}, 0) \\ 0 \end{pmatrix}. \tag{28}$$

We have shown previously [4] that

$$U_{ls}(t) = f(t) + g(t)(\boldsymbol{l} \cdot \boldsymbol{\sigma}) \tag{29}$$

with the following operators

$$f(t) = \mathrm{e}^{\mathrm{i}\frac{t}{2}} \left(\cos \Omega \frac{t}{2} - \frac{\mathrm{i}}{\Omega} \sin \Omega \frac{t}{2} \right) \tag{30}$$

$$g(t) = \mathrm{e}^{\mathrm{i}\frac{t}{2}} \left(-\frac{2\mathrm{i}}{\Omega} \sin \Omega \frac{t}{2} \right) \tag{31}$$

$$\Omega|lm\rangle = \sqrt{1 + 4\hat{l}^2}|lm\rangle = (2l + 1)|lm\rangle. \tag{32}$$

$U_0(t)$ transforms $\boldsymbol{R}_0$ into $\boldsymbol{R}_t$ while $U_{ls}(t)$ acts on the spherical harmonics present in the $\psi_l^m(\boldsymbol{r},t)$. The result is

$$\tilde{\psi}_{\boldsymbol{R}_t}(\boldsymbol{r}) = \mathrm{e}^{[-\mathrm{i}(\frac{3}{2}t+\frac{r_t\cdot p_t}{2})-\frac{r^2+r_t^2}{2}-\frac{E_0}{2}]} \times \sum_{lm} C_{lm}(\boldsymbol{R}_0) W_l(R_t r) \begin{pmatrix} (f_l + m g_l) Y_l^m(\theta,\varphi) \\ \frac{1}{2} g_l \sqrt{l(l+1)-m(m+1)}\, Y_l^{m+1}(\theta,\varphi) \end{pmatrix} \tag{33}$$

where $f_l(t)$ and $g_l(t)$ are simply obtained from (30) and (31) by replacing Ω by $(2l+1)$. This expression corresponds to the most general initial condition with the assumed initial spin direction. The presence of the time dependence in functions f and g from one hand, the presence of Y_l^{m+1} in the lower part of the spinor are the two differences which change the time evolution in an appreciable manner in the case where $\kappa \neq 0$.

We now want to concentrate our efforts on the evolution of a wavepacket which is cylindrically symmetric around Oz for $t = 0$. We assume therefore (denoting unit vector in the Oz-direction by $\hat{z}$)

$$\boldsymbol{r}_0 = -r_0\hat{z} \qquad \boldsymbol{p}_0 = 0 \qquad R_0 = r_0 \tag{34}$$

$$E_0 = \frac{r_0^2}{2} \qquad \theta_{R_0} = \pi \qquad \varphi_{R_0} = 0 \tag{35}$$

$$C_{lm}(\boldsymbol{R}_0) = \delta_{m0}(-1)^l 2\pi^{-\frac{1}{4}} \mathrm{e}^{-\frac{N}{2}} \sqrt{2l+1}. \tag{36}$$

Let us study the sign of the product $C_{l0}(\boldsymbol{R}_0)Y_l^0(\theta,\varphi)$ along the Oz-axis, i.e. $\theta = \pi$ and $\theta = 0$. One has

$$Y_l^0(\pi,0) = (-1)^l \sqrt{\frac{2l+1}{4\pi}} \tag{37}$$

$$Y_l^0(0,0) = \sqrt{\frac{2l+1}{4\pi}}. \tag{38}$$

All the partial waves interfere constructively in the direction $\theta = \pi$ while there is a destructive interference for $\theta = 0$. We also know that there is a radial concentration of the wavepackets shown on figure 2. This explains mainly the known result that the wavepacket is initially a Gaussian centred at $\boldsymbol{r}_0 = -r_0\hat{z}$.

In the direction $\theta = \frac{\pi}{2}$ we have

$$Y_l^0\left(\frac{\pi}{2},0\right) = 0 \qquad \text{if } l \text{ is odd} \tag{39}$$

while for l even its sign is $(-1)^{\frac{l}{2}}$. A destructive interference between the even states is also predicted on the xOy-plane with a different character as for the $+Oz$-direction.

We will now try to repeat these arguments for $t \neq 0$ for each component of the spinor (33). For the part with $s_z + \frac{1}{2}$ we must find the phase of the product $C_{l0}Y_l^0(\theta,\varphi)f_l(t)$. At a time $t = \frac{T_{ls}}{4} = \frac{\pi}{2}$ (assuming $\kappa = 1$) we have for high l:

$$f_l\left(\frac{\pi}{2}\right) \approx \mathrm{e}^{\mathrm{i}\frac{\pi}{4}} \cos(2l+1)\frac{\pi}{4} = \mathrm{e}^{\mathrm{i}\frac{\pi}{4}} \frac{\sqrt{2}}{2}(-1)^{\frac{l}{2}}. \tag{40}$$

The constructive interference of the product considered is now obtained for $\theta = \frac{\pi}{2}$ and for even l. It is interesting to see that the part with $s_z = +\frac{1}{2}$ still has cylindrical symmetry around Oz but, moreover, if $t = \frac{T_{ls}}{4}$ or 0 we shall have the result of figure 2, i.e. a high radial concentration of the wave. One readily understands that at this time the wave is highly peaked on a vortex of radius r_0 with symmetry around Oz, the smaller radius of the vortex being roughly the initial radial spread.

As for the part with $s_z = -\frac{1}{2}$, we must discuss the sign of the product $C_{l0}Y_l^1(\theta,\varphi)g_l(t)\times\sqrt{l(l+1)}$ also for $t=\frac{\pi}{2}$ and for $\theta=\frac{\pi}{2}$. Now $Y_l^1(\frac{\pi}{2},\varphi)=0$ if l is even, its sign for odd l is $(-1)^{\frac{l-1}{2}}$ while $g_l(\frac{\pi}{2})$ has also this sign since

$$g_l\left(\frac{\pi}{2}\right) = -\mathrm{e}^{\mathrm{i}\frac{\pi}{4}}\frac{2\mathrm{i}}{2l+1}\sin(2l+1)\frac{\pi}{4} = \frac{-2\mathrm{i}}{2l+1}(-1)^{\frac{l-1}{2}}\mathrm{e}^{\mathrm{i}\frac{\pi}{4}}\frac{\sqrt{2}}{2}. \tag{41}$$

However, we have also $Y_l^1(\theta,\varphi)\approx \mathrm{e}^{\mathrm{i}\varphi}$. In the case of the part with $s_z=-\frac{1}{2}$ it is the odd partial waves which produce a vortex similar to the part with $s_z=+\frac{1}{2}$ in the limit of high l. A difference occurs in a φ-dependent phase.

For intermediate values of time it is not possible to provide a similar discussion. However, by continuity we can understand that the vortex rings are created from the spherical initial wavepacket and get their full extension for the configuration and at the time chosen.

5. Numerical simulation of the vortex rings

The manifestation of the vortex rings depends on the parameter κ. It is simpler to freeze the evolution under U_0 and to consider only the spin–orbit evolution to begin with in order to emphasize the effect. Figures 3 and 4 represent the density of the full wavepacket at various times on planes yOz and xOz, respectively. Here also we have considered the wavepacket which was analysed in figure 2. (For convenience the spin direction is $s_x=+\frac{1}{2}$

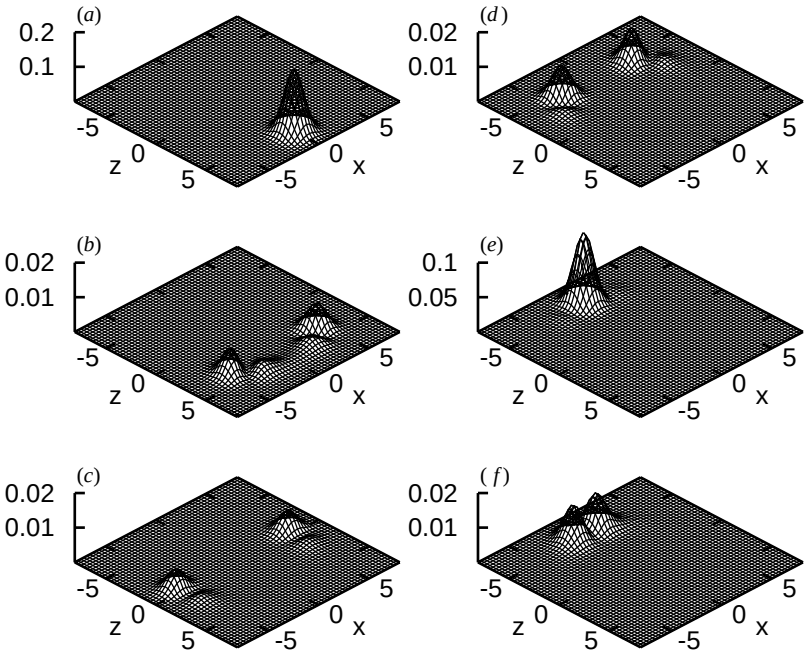

Figure 3. Time evolution of the wavepacket with spin under $U_{ls}(t)$ operator only (evolution according to U_0 is frozen). Shown is the $|\Psi(t)|^2 = |\Psi_+(t)|^2 + |\Psi_-(t)|^2$ as a function of coordinates on the plane xOz. Case $N=20$. Note different vertical scales. Cases *a,b,c,d,e,f* correspond to $t_i = 0, \frac{1}{8}, \frac{2}{8}, \frac{3}{8}, \frac{15}{32}$ and $\frac{4}{8}T_{ls}$ respectively.

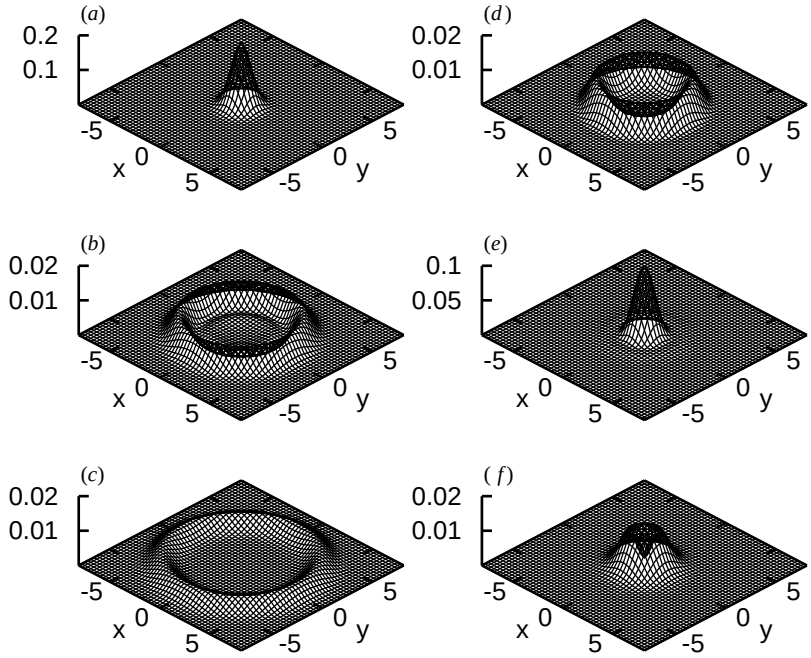

Figure 4. The same wavepacket as in figure 3. Cuts are shown through planes perpendicular to the classical trajectory (Oz-axis) with $z_i = z_0 \cos t_i$ showing explicitly a toroidal shape. Time instants as in figure 3.

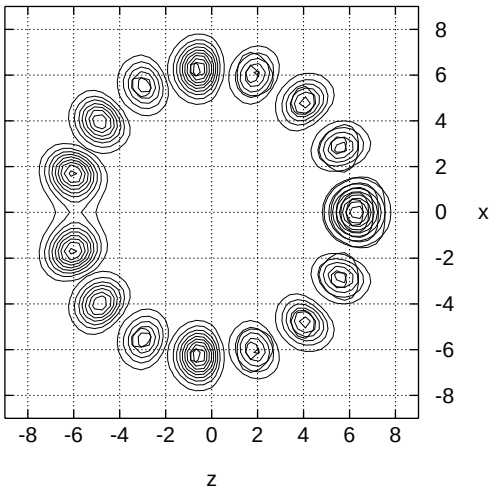

Figure 5. Contour plots of the same evolution as in figure 4, showing that centres of the vortex rings evolve approximately on a sphere with the radius r_0. Here packets corresponding to different time instants are collected in the same picture.

and $\boldsymbol{r}_0 = r_0\hat{x}$ at time $t = 0$.) At time $t = 0$ a Gaussian is represented. At time $t = \frac{T_{ls}}{8}$ a vortex ring is created and gets the maximum radius at $t = \frac{T_{ls}}{4}$ when intersecting the plane yOz. Moreover, figure 4 shows that even a second vortex with a smaller amplitude has also been created that we cannot explain in simple terms. At time $t = \frac{3T_{ls}}{8}$ the vortex ring has a decreasing radius and is centred on a point with $x < 0$. Finally, at time $t = \frac{T_{ls}}{2}$, the wavepacket reassembles near a point with $\boldsymbol{r}_0 = -r_0\hat{x}$. At this time we have shown

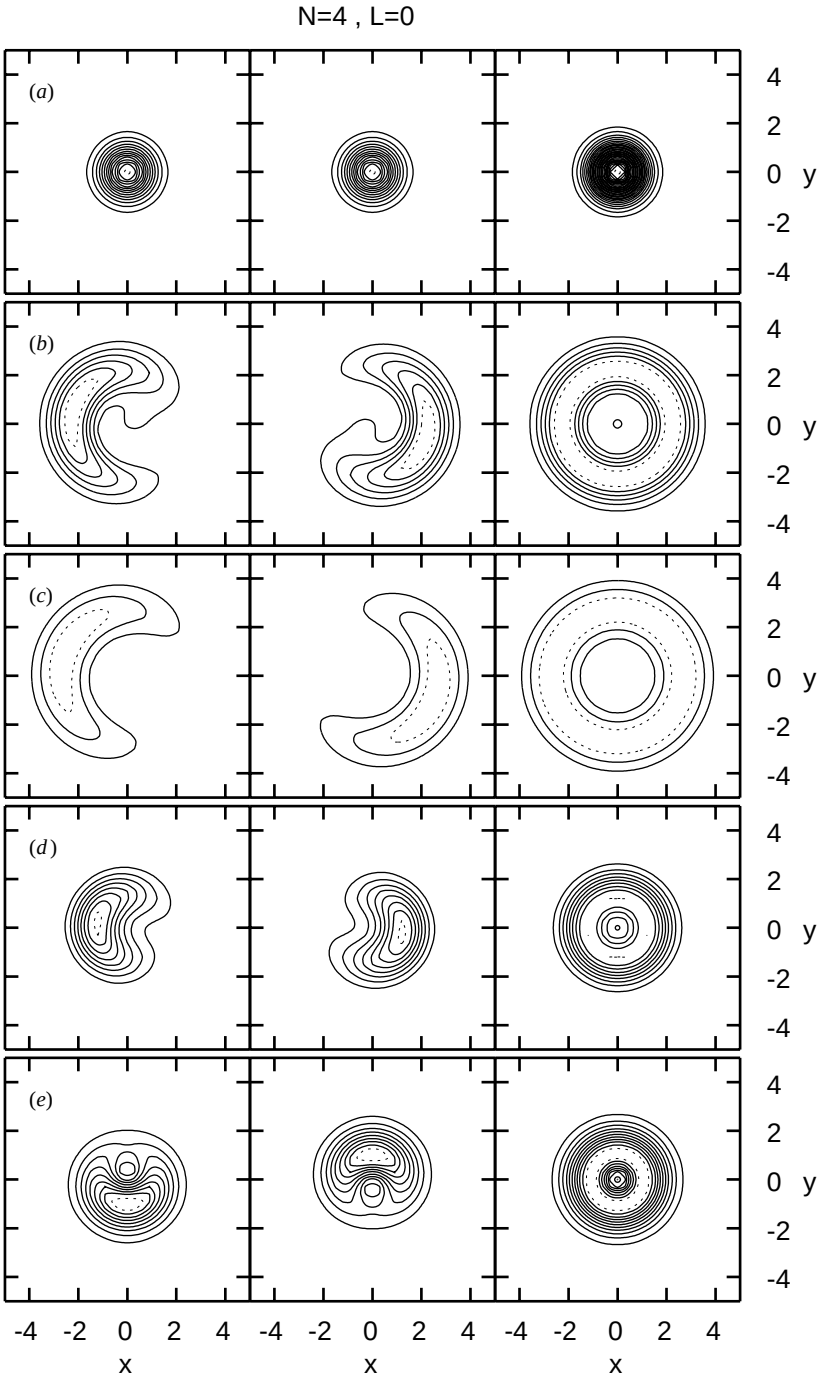

Figure 6. Contour plots showing the decomposition of the total wavepacket (right column) into parts with the opposite spin field (left and central columns). Case $N = 4$. Top row (a) corresponds to $t = 0$, bottom (e) to $t = \frac{1}{2}T_{ls}$. Time steps are $\Delta t = \frac{1}{8}T_{ls}$.

in our previous papers that the spin is approximately reversed. Finally, the behaviour for $T_{ls}/2 < t < T_{ls}$ has not been shown for it is totally reversible if we assume a frozen oscillator.

The vortex rings evolve approximately on a sphere. The intersections of the wavepacket with a plane xOz shown in figure 5 present indeed the feature that the distance to the centre is about r_0 at all times.

Figure 6 shows the decomposition of the toroidal wavepacket into its spin components in a direction perpendicular to the classical motion. The left and central columns display the shapes of subpackets in which the spin field is antiparallel and parallel to the Ox-axis, respectively. Due to symmetry with respect to the Oz-axis (classical trajectory), the similar decomposition with respect to spin components in an arbitrary direction perpendicular to the Oz-axis results in a picture rotated by a certain angle.

6. Conclusions

The dynamics of wavepackets in static potentials implies subtle interference effects which have been beautifully illustrated in the case of Coulomb potential [9–14, 16]. Two general mechanisms have been identified: one is the spread of the wave on the top of a classical trajectory, the other is the regime of partial and also almost complete recurrences. In the case of a pure harmonic oscillator the existence of a single frequency allows a unique interference mechanism of the partial wave that leads to a dispersionless coherent wavepacket. This is the case where quantum mechanics comes closer to classical mechanics: the dynamics of the density probability is identical to the dynamics of the density distribution of the classical ensemble. This property is expected to be lost if a perturbation is added to the potential. If the perturbation is a spin–orbit potential the dynamics of the problem resembles very much that of the JCM [24]. Two versions [25] of this model exist where the time evolution is exactly periodic in the closest analogy to our model: the Raman coupled model and the two photons JCM. In the harmonic oscillator with spin–orbit the dynamics is, however, richer if one follows the angular evolution with different initial conditions. We have previously shown [19] that the amount of partial revival for half a spin–orbit period depends indeed on these conditions. We have extensively discussed [18, 21] cases where the wavepacket is divided into two parts which rotate in opposite directions on a circular average trajectory in much the same way as the Stern–Gerlach effect. In this paper we have shown a new dynamical behaviour for cylindrically symmetric initial conditions: vortex rings are created and destroyed periodically. In a way there is a case where the constructive interference of the wave is kept for the r and θ coordinates but where the spread is applied only to the ϕ variable. It is an open question whether this effect relies only on the properties of the partial waves of the harmonic oscillator discussed in this paper.

Acknowledgment

PR would like to express his thanks to ISN, Grenoble for kind hospitality during his stay in June–July 1996, when much of this work was done.

References

[1] Alber G and Zoller P 1991 *Phys. Rep.* **199** 231
[2] Garraway B M and Suominen K-A 1995 *Rep. Prog. Phys.* **58** 365
[3] Jaynes E T and Cummings F W 1963 *Proc. IEEE* **51** 129

[4] Buck B and Sukumar C V 1981 *Phys. Lett.* **81A** 132
[5] Knight P L 1986 *Phys. Scr.* T **12** 51
[6] Gea-Banacloche J 1990 *Phys. Rev. Lett.* **65**
Gea-Banacloche J 1991 *Phys. Rev.* A **44** 5913
Gea-Banacloche J 1992 *Opt. Commun.* **88** 531
[7] Averbukh I S 1992 *Phys. Rev.* A **46** R2205
[8] Brown L S 1973 *Am. J. Phys.* **41** 525
[9] Parker J and Stroud C R Jr 1986 *Phys. Rev. Lett.* **56** 716
[10] Averbukh I S and Perelman N F 1989 *Phys. Lett.* A **139** 449
Averbukh I S and Perelman N F 1989 *Zh. Eksp. Teor. Fiz.* **96** 818 (Engl. transl. 1989 *Sov. Phys.–JETP* **69** 464)
Averbukh I S and Perelman N F 1991 *Usp. Fiz. Nauk* **161** 41 (Engl. transl. 1991 *Sov. Phys.–Usp.* **34** 572)
[11] Dačic-Gaeta Z and Stroud C R Jr 1990 *Phys. Rev.* A **42** 6803
[12] Peres A 1993 *Phys. Rev.* A **47** 5196
[13] Wals J, Fielding H H and van Linden van den Heuvell H B 1995 *Phys. Scr.* T **58** 62
[14] Bluhm R and Kostelecky V A 1995 *Phys. Lett.* A **200** 308
[15] Abramowitz M and Stegun I A 1964 *Handbook of Mathematical Functions* (Washington, DC: National Bureau of Standards) section 10.2
[16] Boris S D, Brandt S, Dahmen H D and Stroh T 1993 *Phys. Rev.* A **48** 2574
[17] Cohen-Tannoudji Diu C B and Laloe F 1977 *Mécanique Quantique* (Paris: Herman) p 570
[18] Arvieu R and Rozmej P 1994 *Phys. Rev.* A **50** 4376
[19] Arvieu R and Rozmej P 1995 *Phys. Rev.* A **51** 104
[20] Rozmej P and Arvieu R 1996 *J. Phys. B: At. Mol. Opt. Phys.* **29** 1339
[21] Rozmej P and Arvieu R 1996 *Acta Phys. Pol.* B **27** 581
[22] Rozmej P, Berej W and Arvieu R 1997 *Acta Phys. Pol.* B **28** 243 (invited talk at *XXXI Zakopane School of Physics (September 3–11, 1996)*)
[23] Mikhajlov V V 1973 *Izv. Akad. Nauk SSSR, Ser. Fiz.* **37** 2230 (Engl. transl. 1974 *Bull. Acad. Sci. USSR, Phys. Ser.* **37** 187)
[24] Shore B W and Knight P L 1993 *J. Mod. Opt.* **40** 1195
[25] Phoenix S J D and Knight P L 1990 *J. Opt. Soc. Am.* B **7** 116